

Kinematics of the Dena Fault and Its Relation to Deep-Seated Transverse Faults in Zagros Fold-Thrust Belt, Iran

F. Shabani-Sefiddashti and A. Yassaghi*

*Department of Geology, Faculty of Sciences, Tarbiat Modares University,
P.O. Box 14115-175, Tehran, Islamic Republic of Iran*

Received: 21 June 2010 / Revised: 22 May 2011 / Accepted: 6 August 2011

Abstract

The NNW-trending Dena Fault, with 140 km length, cuts the major structures of Zagros Fold-Thrust Belt in Borujen region. The fault has divided the region in two zones, in which different structural, and morphological features as well as sedimentation and seismotectonic characteristics have developed. This study presents a new interpretation for the kinematics of Dena Fault based on field evidence. Precise field mapping and structural analysis in four structural traverses across the Dena fault zone indicates that it composes of several sub parallel surface fault segments with right-lateral strike-slip to reverse right-lateral fault mechanism. Coincidence of the Dena Fault with the T-11 aeromagnetic lineament as well as evidence on the fault activity on isopach maps from Cretaceous to Miocene time implies that the north segment of the Dena Fault has kinematics relation to this lineament. The low angle between the general trending of the mapped fault segments on the surface with the trend of the aeromagnetic lineament implies their close relationship. Therefore, it is proposed that the mapped fault segments are the Riedel shear faults of an active deep-seated strike-slip fault on the surface. In addition, the proposed kinematics for the Dena Fault is compatible with the focal mechanism of earthquakes epicentered along the fault. The result of this interpretation documents that the Dena Fault is a basement fault with right-lateral strike-slip mechanism.

Keywords: High Zagros; Dena Fault; Fault geometry and kinematic; Aeromagnetic Lineament; Fault segments

Introduction

The NNW-trending Dena Fault extends from the south of the Borujen city to the northwest of Yasouj city

(Fig. 1). The fault crosses both the High Zagros and Folded Belt zones of Zagros from North to South. The northern portion of the fault, transversely, separates the High Zagros zone in Borujen area to different structural,

* Corresponding author, Tel.: +98(21)82883406, Fax: +98(21)82884435, E-mail: yassaghi@modares.ac.ir

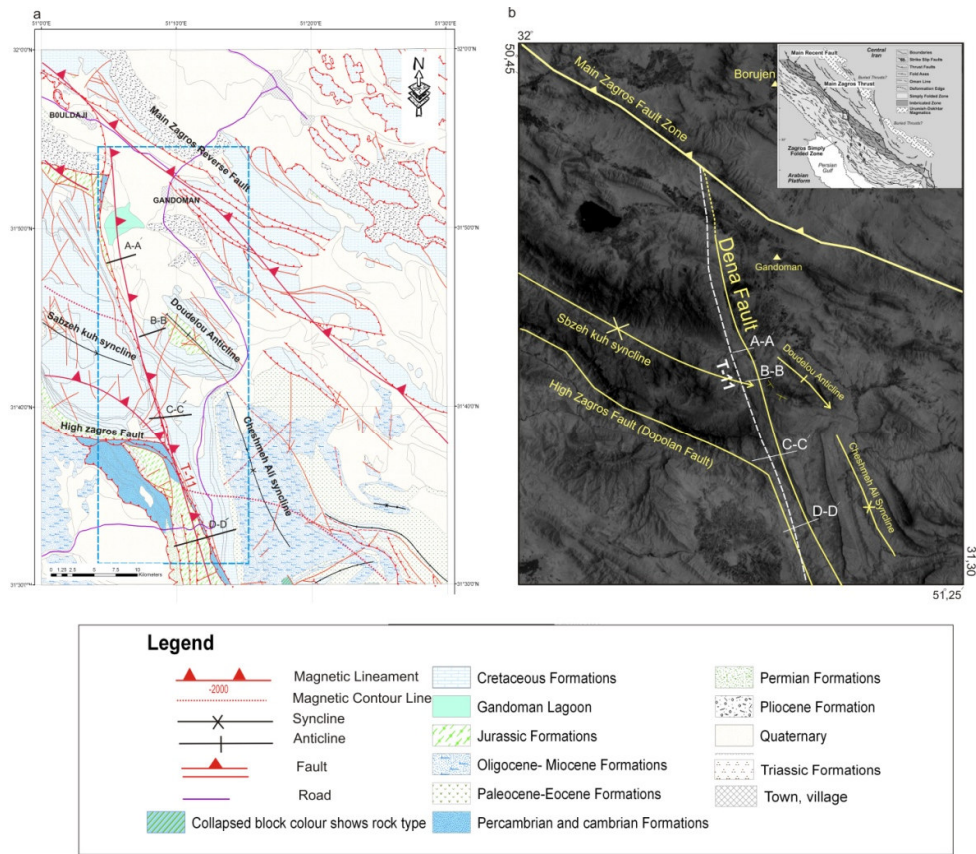


Figure 1. Location map of the Dena Fault and the surrounding structures; (a) Interpreted structural map (after [3]); (b) 6-band Landsat image. Position of the traverse lines, perpendicular to fault trend and T-11 magnetic lineament [9] is also shown.

seismotectonics and geomorphology distinct.

In the aeromagnetic map of Semirom, basement in the western part of the Dena Fault located at the depth of ten Km while in the eastern part of the fault it is deepened at five Km [1]. In addition, Jurassic formations have exposed to the surface in the eastern part of the fault, whereas they have buried to depth of five Km in the western part of the fault [2]. Therefore, basement and overlying cover sequence have risen to upper structural level in the eastern part of the Dena Fault. Previous studies show that the Dena Fault has acted in two different mechanisms. Some authors [e.g. 3] believes that the Dena Fault have acted as a dextral strike-slip fault in the Cambrian, but have been reactivated to reverse mechanism in the Quaternary. In contrast, others [4,5] noted that the older activity of the Dena Fault was reverse, with movement direction toward the west, but its present activity is strike-slip fault. In addition, Alavi [6] noted that Dena Fault is east

dipping and show right-lateral reverse mechanism, while Berberian [7] believes that activation of the Dena fault zone resulted in major facies variations in region. Moreover, microearthquake seismicity indicates that slip associated with the Dena Fault is right-lateral strike-slip [8].

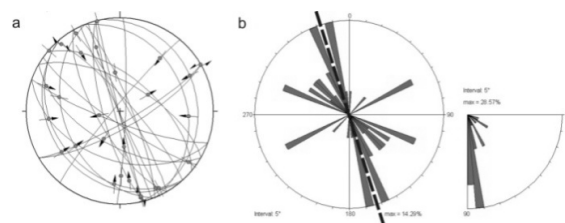


Figure 2. Stereograms show (a) the geometry and kinematics and (b) rose diagram on trend of the main faults along the Dena Fault. Note to trend of the T-11 aeromagnetic lineament shown as dashed line.

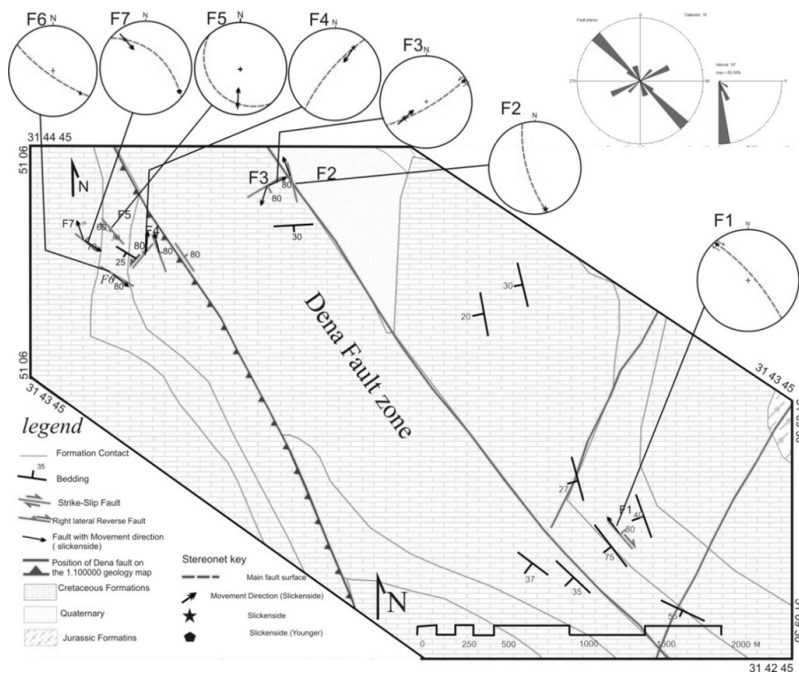


Figure 3. Structural map of the B-B' traverse. Note to stereograms on kinematic of the mapped faults in this traverse which almost all show mainly strike-slip faults.

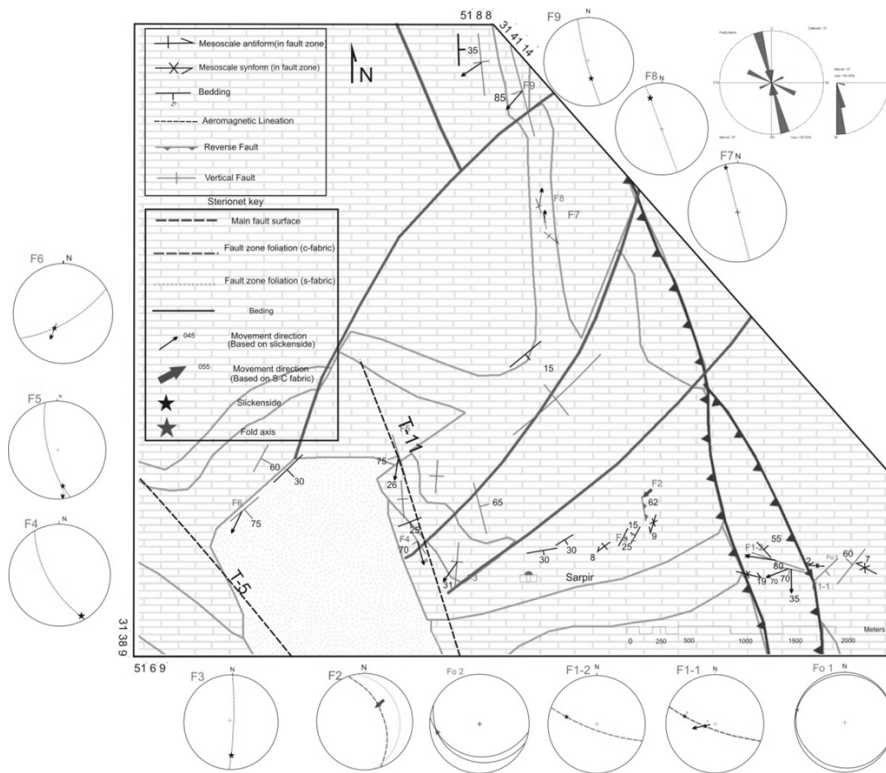


Figure 4. Structural map of the C-C' traverse. Note to stereograms on kinematic of the mapped faults in this traverse which almost all show mainly strike-slip faults.

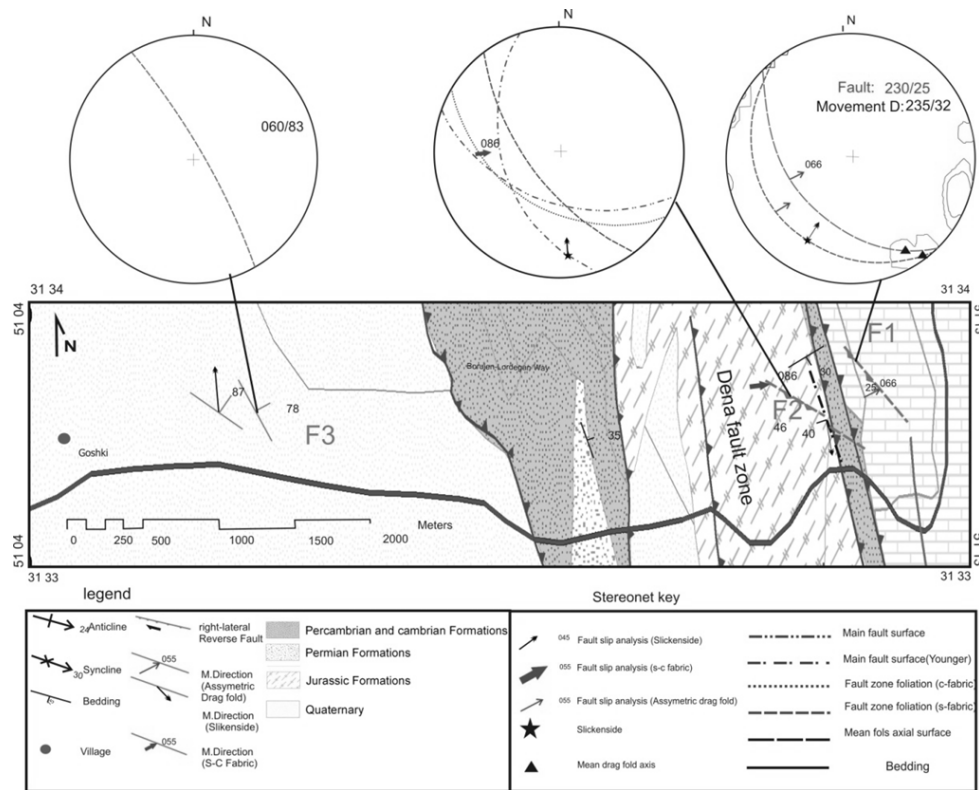


Figure 5. Structural map of the D-D' traverse. Note to stereograms on kinematic of the mapped faults in this traverse which almost all show mainly reverse faults.

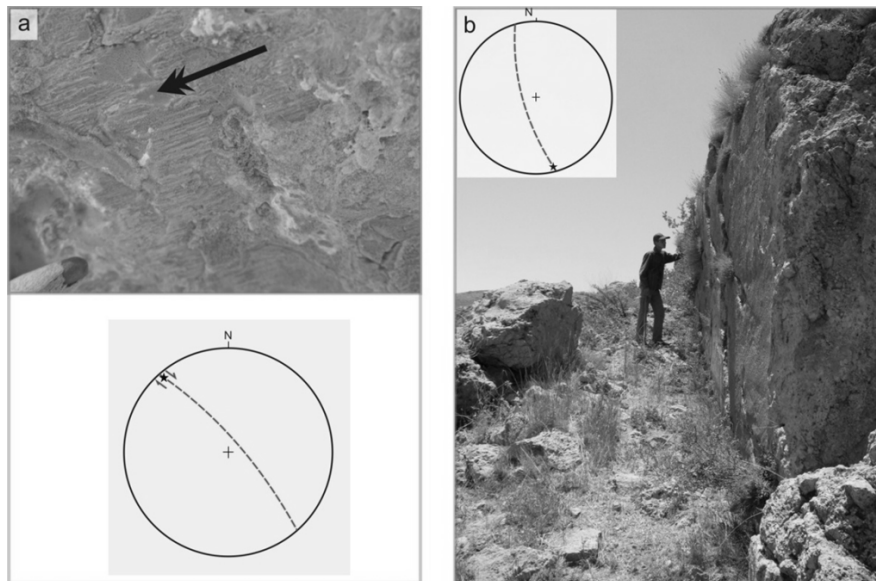


Figure 6. Photographs and stereograms show fault surface and kinematic interpretation of (a) The F1 and (b) The F2 fault in the B-B' traverse. Note to dextral strike-slip kinematics for both faults.

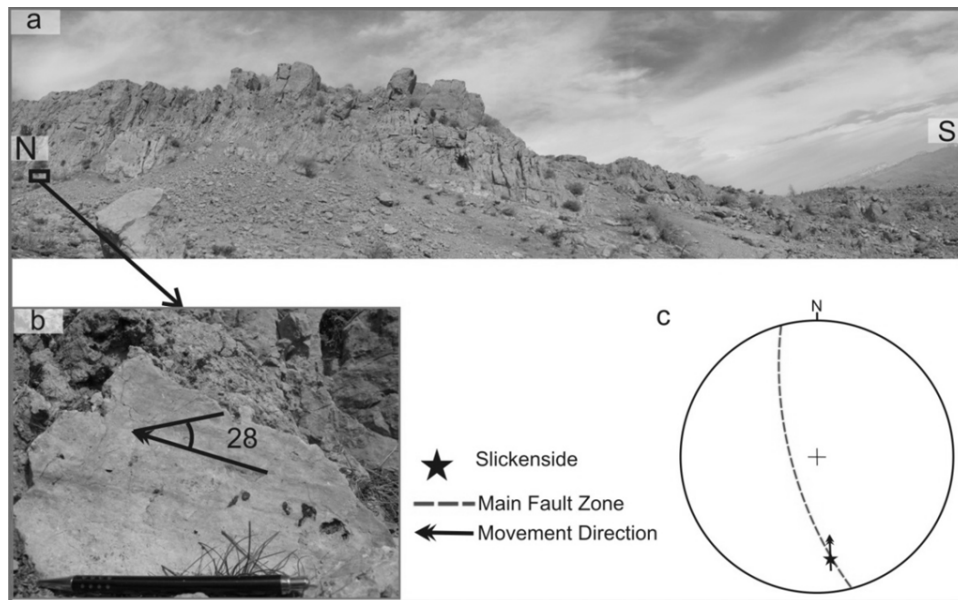


Figure 7. Photography of (a) Fault zone and (b) Fault surface of the F1 along the C-C' traverse.

Since different ideas have presented as to the Dena fault zone mechanism, this paper is attempt to present detailed structural analysis of the Dena Fault in Borujen area using four traverses across the fault zone to unravel geometry and kinematics of the fault. To document the fault origin, the relationship between the mapped surface faults and subsurface basement faults, using aeromagnetic and isopach maps, is also analyzed.

Materials and Methods

Structural Features of the Dena Fault Zone

The reliable approach on recognizing deformation pattern of structural zones can be done using geometric and kinematic analyses of deformed structures (folds and faults). Structural elements such as fault slickenside surfaces, asymmetrical folds and S-C structures are common indicators for kinematic analysis of fault zones [e g 10]. Mapping of the Dena fault zone structures has carried out in four traverses perpendicular to the fault trend (Figure 1). However, geometry and kinematics of the fault across three of the traverses (D-D' and C-C' and B-B') are presented in detail in this section.

Distribution of faults trends and kinematics in the traverses show that three fault set as 1) NNW-trending, 2) WNW- trending and 3) ENE- trending have been mapped in the fault zone (Figure 2). The majority of the faults are steeply dipping (more than 80 degrees).

The NNW-trending faults, such as the F1 and F2 faults in the B-B' traverse (Figures 3 and 6) and the F5 fault in the C-C' traverse (Figures 4 and 7), have high dip angle to both east and west directions. Based on stereographic analysis of the fault-slip lines, the fault kinematics varies from strike-slip to oblique-slip motion with dominant strike-slip component. The close relations between these faults trends with the trend of the T-11 aeromagnetic lineament (Figure 2) imply their possible kinematic relation.

The ENE- trending faults with high dip angle (80-8), such as the F5 fault in the B-B' traverse (Figure 3 and 8), indicate the left lateral kinematics.

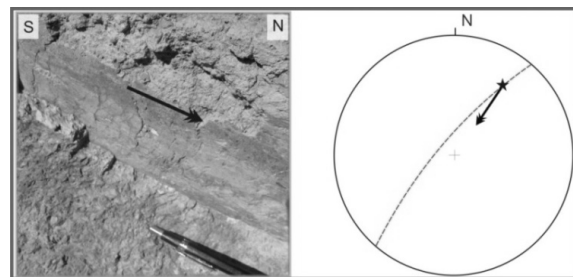


Figure 8. Photograph of the F5 Fault surface in the B-B' traverse. The stereogram shows left-lateral strike-slip kinematics using steps on the fault surface.

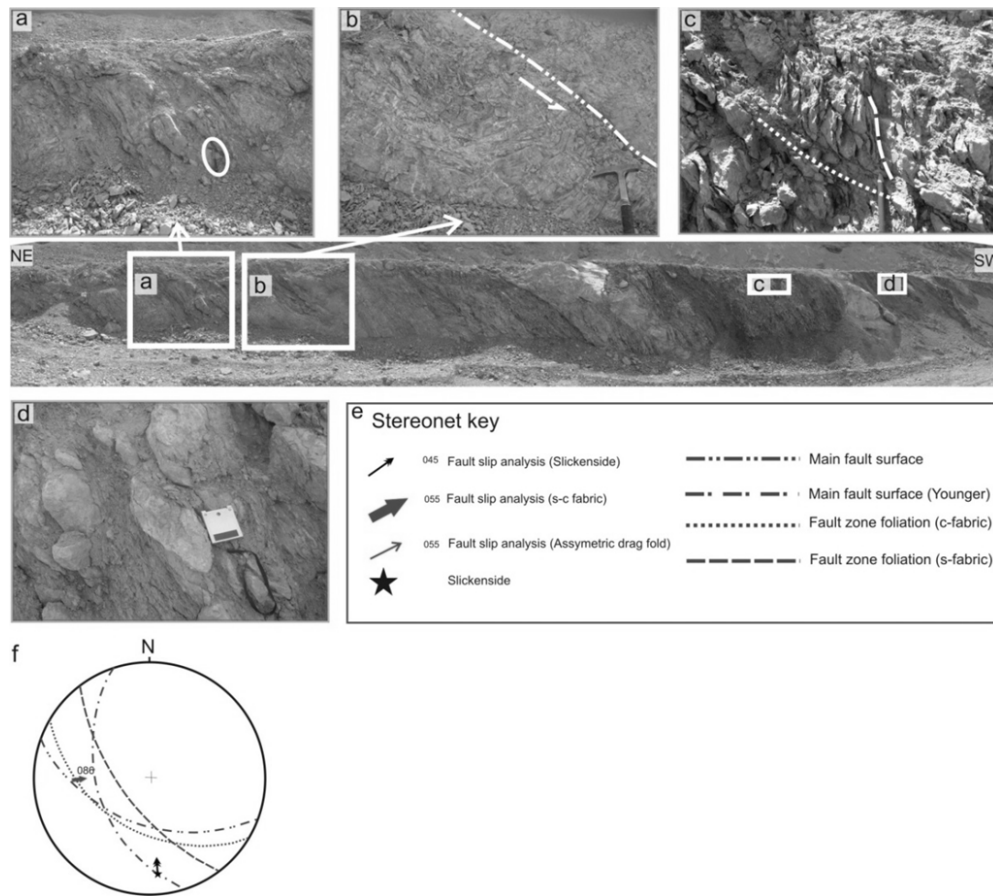


Figure 9. Photographs of structures developed in the F2 fault zone in the D-D' traverse. (a) Duplexes formed in the fault zone. (b) Footwall syncline. (c and d) S-C structures developed in the fault zone. (f) Stereonet show reverse kinematics for the fault.

Kinematics of the WNW- trending fault zones are detected using S-C structures [11] Figures 9c and d), fault related duplexes (Fig. 9a), and fault-related folds (Fig. 9b) [12]. They indicate reverse or reverse with left-lateral component kinematics for these faults (Fig. 9). The dip angle of the faults varies from 25-60 degrees (for example F2 fault in the D-D' traverse as shown in Figure 5 and 9).

Results and Discussion

Dena Fault Kinematics

The Dena Fault in most previous studies is defined as the northern part of the Kazerun Fault. The Zagros fold thrust belt is crossed by several NNW-trending transverse right-lateral strike-slip faults as Kazerun, Karebass, Sabzpushan and Sarvestan faults [e.g., 13-

15]. There are different ideas about geometry and kinematics of the Dena Fault. As to the fault geometry, Sedaghat [3] believes that the fault is dipping towards the west. However, Almasiyan [1] suggests that the fault is dipping towards the east. Nevertheless, as to temporal evolution of the Dena Fault, it is believed that the fault has acted as a reverse fault with movement direction towards the west until the Late Pliocene, but its present activity is strike-slip [4,5]. Detailed structural analysis in this study shows that majority of the minor faults in the Dena fault zone striking from north-northwest to west-northwest and dipping to different SW and NE directions. These minor faults based on measured and or interpreted movement directions (Figures 6 and 7) show dextral strike-slip to dextral oblique slip kinematics. Therefore, the interpreted geometry and kinematics of these minor faults from the Dena Fault in this study (Figures 6 and 7) imply a dextral strike-slip kinematics

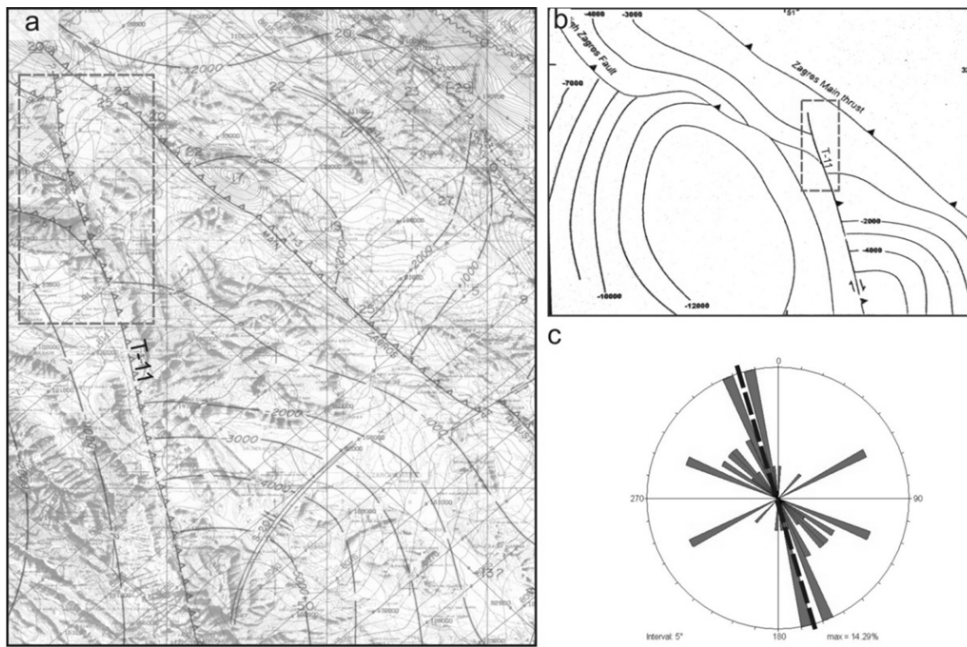


Figure 10. (a) Location of the study area and T-11 lineament on aeromagnetic map of Semirum (after [1]). (b) Subsurface contour map of the basement based on magnetic data. Rectangle shows the location of the study area. (c) Trending rose diagram of faults in the fault zone is compared with aeromagnetic lineament trend.

for the fault zone. Earthquake focal mechanisms epicentered along the fault zone are compatible with the interpreted kinematics for the Dena Fault [9].

The Origin of the Dena Fault and Its Relationship with Basement Structures

In the absence of magmatic activity, or of the deposition of sediments containing significant magnetic minerals since the Paleozoic in the Zagros, the source of the observed magnetic anomalies (Fig. 4a) are considered to be due to the effect of tectonics fabrics in the crystalline basement [14,15].

The presences of anomalies in the isomagnetics intensity lines of the Semirum aeromagnetic map reveal an obvious magnetic lineament (T-11 lineament in Figs 10a and 10b). The statistical rose diagram of the minor faults in the Dena fault zone show that there is a good correlation between their trends with the trend of the T-11 lineament (Figure 10). Comparison of the general trend of the mapped dextral slip faults with the T-11 aeromagnetic lineament, indicate that they have very low azimuth angle variation (Figure 12c). The geometric relation between the mapped faults on the surface with the magnetic lineament implies the kinematic relationship between these structures.

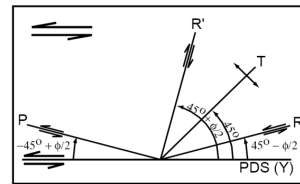


Figure 11. Idealized Riedel shear zone geometry. ϕ is the angle of internal friction of the host rock (after [3]).

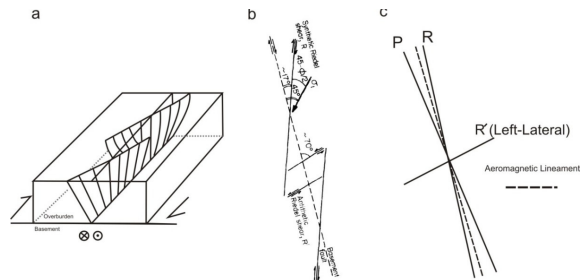


Figure 12. (a) Helicoidal form of individual Riedel shears in right-lateral simple shear, (redraw from [17]). (b) Minor strike slip faults developed above a dextral strike-slip basement fault [17] (c) The general trend of majority-detected faults in the Dena fault zone and their relationship with regional aeromagnetic lineament have indicated. Please attend to trend of T-11 basement fault.

Experimental studies on movement along basement faults overlaid by viscous material like salt [16] showed that reactivation of the basement faults could not cut the overlying thick material and then do not emerge to the surface. Their reactivation, however, produces a pattern of an echelon faults and folds on the cover sediments [17]. Thus, the presence of the Hormoz salt overlain the Zagros basement influences on the activity of deep-seated basement faults such as the Dena Fault and resulted in development of an echelon pattern of faults on the cover surface. Continuation of the basement fault activity at depth is resulted in development of Riedel type shear faults as R, R', P and T type faults on the cover surface (Figure 11). Propagation of shears as the Riedel shear zone may also induce local stress field rotation, further influencing the types and geometry of developing shear fractures [e.g. 17].

Typical Riedel shears show concave upwards shape that diverging from the basement fault and forming a 'Tulip structure'. R fractures have helicoidal shape in three dimensions (Figure 12 A).

Comparison between detected structures in the Dena fault zone with the presented model in figure 11 shows that fractures in the fault zone can be proposed as the younger orders of fractures resulted from the continuation of the Dena Fault activity at depth. Thus, the NNW-trending en-echelon faults (Fig. 12 b) are compatible with R Riedel shear faults (Figs 12a and c). Similarly, the ENE-trending faults with left-lateral slip kinematics can be considered as R' type of Riedel shear faults that resulted from the Dena Fault activity at depth.

A few degrees difference between the attitudes of the mapped faults in the Dena fault zone with the presented model in Figure 11 is interpreted to occur due to different orders of Riedel shear fractures or inactive rotation of structures during the younger activity.

The presented interpretation as to relationship between the mapped structures along the Dena fault zone and the regional aeromagnetic lineament, poses as a basement fault, need further subsurface investigation.

Dena Fault Activity Time and Its Relationship with the Zagros Structures

The axial surface trace of folds in Zagros fold-thrust belt change when they cross the transverse faults [18-20]. For instance, folds outside the Dena fault zone have axial surface traces of 130-trending in Azimuth, whereas when they cross the fault zone their axial surface traces changes to Azimuth of 145 as a clockwise sense of rotation such as the Sabzehkuh Syncline and the Doudelou Anticline (Figure 1). In addition, Evidence on right lateral offset of river channels (Figure

13) demonstrates activity of the fault zone even since Late Miocene when the Zagros fold-thrust belt is evolved. Evidence on passive rotation of the folds axial surface traces sub parallel to the Dena Fault trend such as the Cheshmeh Ali Syncline (Figure 1) also constrain the temporal activity of the fault zone.

Similarly, study of published isopach maps of Zagros show evidence of the Dena Fault activity along a linear structure with N-NW trend from Cretaceous to Miocene (Fig. 14). These imply the influence of the fault on sedimentation control of the region during the time.

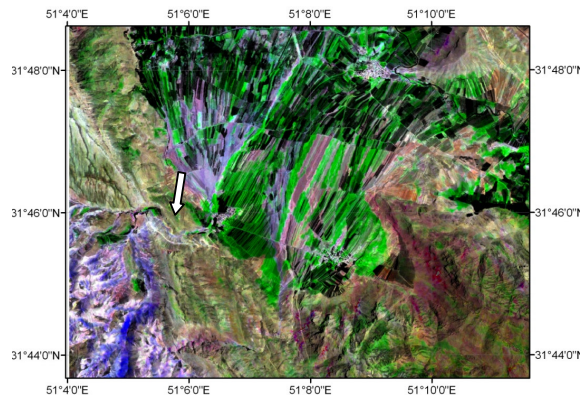


Figure 13. Show right lateral offset of a river channel along the Dena Fault Zone.

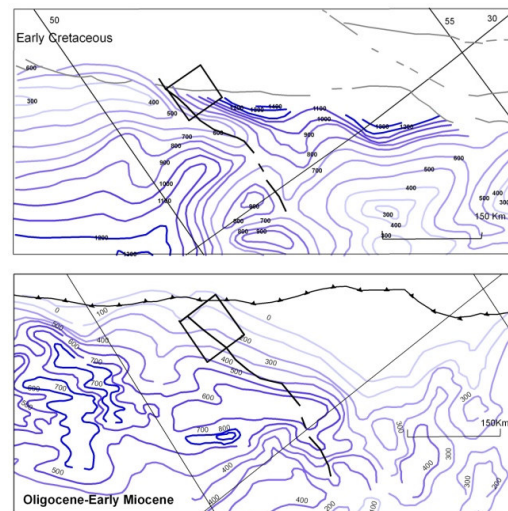


Figure 14. Isopach maps of the Zagros rock formation from the early Cretaceous and Oligocene-early Miocene show thickness variation in the Zagros (after [21 and 22]). Note to the Dena Fault trend shown by solid line.

In conclusions, detailed field mapping integrated with satellite images of the region show that, in addition to compression activity, the Dena Fault has strike-slip movement. Evidence, such as right lateral offset of river channels and clockwise rotation of the west flank of the Doudlo anticline and its displacement along the fault indicate the younger strike-slip mechanism for the Dena Fault. Coincidence of the Dena Fault trend with the T-11 magnetic lineament as well as evidence of the Dena Fault activity, on the isopach maps from Cretaceous to Miocene, show the fault is a deep-seated basement structure. The low angle between the general trend of the mapped faults in the Dena Fault zone with this magnetic lineament imply that these fault were more likely developed as Riedel shear fractures resulted from a basement fault activity on the surface. The presence of the Hormoz salt overlain the Zagros basement though prevent the influence of the Dena Fault on surface but causes development of younger Riedel shear fractures with an echelon pattern on the sedimentary cover. Comparison of experimentally pattern of such faults with mapped faults in the Dena fault zone shows the NNW- trending faults are R and P type faults while ENE-trending faults are R' type. Coincidence of the Dena Fault kinematics with mechanism of earthquakes epicentered along of the fault zone confirms the basement origin and that of right-lateral kinematics of the Dena Fault since Cretaceous.

References

1. Almasiyan M. Tectonics and seismotectonics of Dena-Zagros tear zone in the Borujen Area, M Sc *Thesis*, Azad University, Tehran, 184 p. (1992).
2. McQuarrie N. Crustal scale geometry of the Zagros fold-thrust belt, Iran *J Struct Geol*, **26**: 519–535 (2004).
3. Sedaghat, M A 1, 100000 Geological map of Burujen, Geological Survey of Iran (1996).
4. Authemayou C., Bellier, O., Chardon, D., Malekzad, Z., and Abbassi, M Role of the Kazerun fault system in active deformation of the Zagros fold- and- thrust- belt (Iran). *C R Geoscience*, **337**: 539-545 (2005).
5. Authemayou C., Chardon, D., and Bellier, O. Late Cenozoic partitioning of oblique plate convergence in the Zagros fold-and thrust belt (Iran). *Tectonics*, **25**: 1-21 (2006).
6. Alavi M., Geological map of Borujen. Geological survey of Iran, scale 1:250000 (1977).
7. Berberian M., and King G.C.P. Towards a paleogeography and tectonic evolution of Iran. *Can. J. Earth Sci*, **18**, 210–265 (1981).
8. Yamini-Fard F., Hatzfeld, D , Tatar, M., and Mokhtari, M. Microearthquake seismicity at the intersection between the Kazerun fault and the Main Recent Fault (Zagros, Iran). *Geophys J. Int*, **166**: 186-196 (2006).
9. Yousefi E., and Friedberg, J.L. Aeromagnetic map of semirom. Scale 1 250000, Geological survey of Iran (1978).
10. Marshak S. and Mitra G. Basic Methods Of Structural Geology. Prentice Hall, 446p. (1988).
11. Hippert J. Are S-C structures, duplexes and conjugate shear zones different Manifestations of the same scale-invariant phenomenon *Journal of Structural Geology*, **21**: 975-984 (1999).
12. Doblás M. Slicken side kinematic indicators *Tectonophysics*, **295**: 187-197 (1998).
13. Hatzfeld D., Authemayou C., Van Der Beek P., Bellier O., Lave J., Oveisi B., Tatar M., Tavakoli F., Walpersdorf A., and Yamini-Fard F. The kinematics of the Zagros Mountains (Iran). Geological Society Special Publication, **330**: 19-42 (2010).
14. Bahroudi A., and Talbot, C.J. The configuration of the basement beneath the Zagros basin. *Journal of Petroleum Geology*, **26**: 257-282 (2003).
15. Morris P. Basement structure as suggested by aeromagnetic surveys in southwest Iran Proceedings of the Second Geological Symposium of Iran, Tehran, Iranian Geological Institute. (1977).
16. Darrell S., Ferrill, D.A. and Stamatakos, J A. Role of ductile decollement in the development of pull-apart basins: Experimental results and natural examples. *Journal of Structural Geology*, **21**: 533–554 (1999)
17. Naylor M A , Mandl, G. and Sijpesteijin, C H K. Fault geometries in basement-induced wrench faulting under different initial stress states. *Journal of Structural Geology*, **8**: 737-752 (1986).
18. Yassaghi A. Integration of Land sat imagery interpretation and geomagnetic data on verification of deep-seated transverse fault lineaments in SE Zagros, Iran. *International of Remote Sensing*, **27**: 4529-4544 (2006).
19. Fürst M. Strike-slip faults and diapirism of the south eastern Zagros ranges. In Proceedings of Symposium on Diapirism, Bandar Abbas, **2**: 149-183 (1990).
20. Hessami K., Koyi, H. A., and Talbot, C. J. The significance of strike-slip faulting in the basement of the Zagros Fold and Thrust belt. *Journal of Petroleum Geology*, **24**: 5-28 (2001).
21. Motiei H. *Geology of Iran - volume 1: stratigraphy of Zagros*. Geological survey of Iran publications, Tehran, 556 p. (1994).
22. Sepehr M. and Cosgrove, J.W. Structural framework of the Zagros fold thrust belt, Iran. *Mar. Pet. Geol*, **21**: 829-843 (2004).